

## PROGRESS ON THE IMP FACILITY\*

D.L. Coffey and W.F. Gauster  
Oak Ridge National Laboratory  
Oak Ridge, Tennessee

The conceptual magnet design of the "IMP" ("Injection into Microwave Plasma") facility of the Oak Ridge National Laboratory has been briefly described as an example of a nonaxisymmetrical superconducting magnet system in a paper which discusses general problems in designing such systems.<sup>1</sup> In the following additional detail will be presented.

The IMP facility consists of two mirror coils surrounded by a quadrupole magnet system ("Ioffe bars") as shown in principle in Fig. 1. The inside diameter of the mirror coils is 18 cm. The field strength in the centers of the mirror coils is 40 kG and that in the center of the entire system is 20 kG. The quadrupole produces an additional magnet field such that the total field increases from the minimum value of 20 kG in the system center to at least 26 kG when one proceeds from the center in any direction ("B-minimum field"). The maximum field strength in the mirror coils is 68 kG, that in the quadrupole is 75 kG.

Figure 2 shows the midplane cross section of the magnet system. The current density in the quadrupole was assumed to be  $11\,300\text{ A/cm}^2$ , that in the mirror coils to be  $10\,600\text{ A/cm}^2$ . In order to provide a free cylindrical opening for the mirror coils, the quadrupole coils were supposed to have saddle shape. Applying the computation methods described at another place,<sup>1</sup> it became obvious that, for a symmetrical quadrupole design as shown in Fig. 2, the space between Ioffe coils (positions  $S_1$  to  $S_4$  in Fig. 2) is especially important for providing ampere turns, i.e., ampere turns at these places of the quadrupole are most effective. When using stainless-steel-reinforced  $\text{Nb}_3\text{Sn}$  ribbons for the quadrupoles, it would be possible to fill out almost entirely the spaces  $S_1$  to  $S_4$  and to make the windings in saddle shape. Such a design of a  $\text{Nb}_3\text{Sn}$  quadrupole has been described by Sampson et al.<sup>2</sup> In the case of the IMP project, the electromagnetic forces on the windings are so high that very strong stainless-steel reinforcement would be necessary, and it would not be possible to reach the desired average current density.

Windings made of NbTi can carry certain hoop stresses and for axisymmetrical magnet systems simple reinforcements, say, in the form of stainless-steel bands, can be conveniently provided if necessary. For nonaxisymmetrical magnet systems, the only practical solution is to encase the magnet windings by strong mechanical structures. In order not to lose precious winding spaces  $S_1$  to  $S_4$  by the walls of the supporting winding cases, it is preferable to provide a nonsymmetrical design as shown in Fig. 3. The computation method used for volume optimization of quadrupole windings is described elsewhere.<sup>1</sup> To build such a quadrupole with saddle-shaped coils would be difficult, and it was decided to provide the simpler "race track" shape (see Fig. 1 of Ref. 1).

---

\* Research sponsored by the U.S. Atomic Energy Commission operated by the Union Carbide Corporation.

1. W.F. Gauster and D.L. Coffey, J. Appl. Phys. 39, 2647 (1968).
2. P.G. Kruger, J.N. Snyder, and W.B. Sampson, J. Appl. Phys. 39, 2633 (1968).

A disadvantage of the race track shape is that the "turn arounds" of the larger quadrupole windings (Coils A and A' and B and B' in Fig. 3) would interfere with the mirror coils if the quadrupole coils did not have sufficient axial length. However, this disadvantage seemed to be not decisive, and the project assumes that the larger quadrupole coils are sufficiently long.

As discussed in Ref. 1, the electromagnetic forces acting on the mirror and the Ioffe coils of the IMP facility are very high. Here, we will not describe in detail the force and stress analysis of the IMP magnet system, but we restrict ourselves to making a few general remarks about problems of this kind.

First, if we assume the use of NbTi for winding the coils, we have to consider the performance of compound conductors made up of two different materials with different Young's (and strictly speaking also Poisson's) moduli and different thermal expansion coefficients. At 77°K, the Young's moduli are<sup>3</sup>

$$E_1 = E_{\text{copper}} = 20 \times 10^6 \text{ psi}$$

$$E_2 = E_{\text{NbTi}} = 12.2 \times 10^6 \text{ psi} .$$

These values are not very different from those at 4.2°K.

When cooling down from room temperature to 4.2°K, the contraction is<sup>4</sup>

$$\frac{\Delta l}{l}_{\text{copper}} = - 326 \times 10^{-5} = \bar{\alpha}_1 \times (4.2 - 300)$$

$$\frac{\Delta l}{l}_{\text{NbTi}} = - 131 \times 10^{-5} = \bar{\alpha}_2 \times (4.2 - 300) .$$

By applying the well-known stress-strain relations, we obtain an equivalent Young's modulus E, and an equivalent average expansion coefficient  $\bar{\alpha}$  as follows:

$$E = \frac{1 + a(e - 1)}{e} E_1 \tag{1}$$

$$\bar{\alpha} = \frac{\bar{\alpha}_1 ea + \bar{\alpha}_2 (1 - a)}{1 + a(e - 1)} \tag{2}$$

Here, the quantities a and e are the ratios

$$a = \frac{\text{cross section area of copper}}{\text{total cross section area}}$$

and

$$e = \frac{E_1}{E_2} .$$

3. D.B. Montgomery, private communication.

4. National Bureau of Standards Nomograph 29.

Using Eqs. (1) and (2), stress and strain of the two components of a compound conductor (which has been prestressed at room temperature and then cooled down) can be calculated as if it were a uniform body.

Unfortunately, at this time insufficient research has been done to enable one to calculate reliable values of the stresses in nonaxisymmetrical coil systems, i.e., in coils of nonaxisymmetrical shape or in axisymmetrical coils exposed to nonaxisymmetrical electromagnetic forces. For instance, the mirror coils of the IMP device are axisymmetric; however, the total electromagnetic forces, considering the fields generated by the Ioffe coils, are not axisymmetric. At the Oak Ridge National Laboratory, approximation methods for treating cases of this kind have been worked out and have been used for designing the mechanical structure of IMP. Here, we will not discuss this rather complicated matter, but we will present only a few related simple problems of a general nature.

The first problem concerns the forces in a wire and on the spool when a coil is wound with stressed wire. No electromagnetic forces are considered. If the spool radius is  $r$  and if friction is not taken into account, the hoop stress  $\sigma$  and the tension  $S$  are

$$S = \sigma A = pr \quad , \quad (3)$$

where  $A$  is the wire cross section and  $p$  the force exerted on the spool per unit length of the wire. If the wire is wound with the tension  $S$  in one layer of  $n$  turns on a spool with the length  $l$ , it could be expected that the pressure  $\sigma_r$  on the spool is

$$\sigma_r = \frac{n}{l} \frac{S}{r} \quad . \quad (4)$$

The assumption of no friction is, however, unrealistic. After Euler's formula, the forces  $S$  and  $S_0$ , acting on the cross sections of a rope which is wound around an angle  $\varphi$  over a spool (Fig. 4), are correlated by

$$S = S_0 e^{f\varphi} \quad , \quad (5)$$

if  $f$  is the coefficient of static friction between rope and spool surface. Practically, it is very difficult to estimate with sufficient accuracy the friction coefficient,  $f$  [which should be known very exactly since  $f$  appears in Eq.(5) in the exponent of an e-power].

The difficulty becomes worse if we try to determine the pressure  $\sigma_r^*$  on the spool surface for the case of a winding with a certain number of layers instead of a single layer. We assume that in the wire the tension  $S$  decreases in some way with increasing distance from the point where the wire leaves the spool during the winding process. We will use a simple model which considers only a relatively small number of layers,  $\gamma$ , stressed, however, with the full wire force  $S$ , and we write

$$\sigma_r^* = \frac{n}{l} \frac{S}{r_{av}} \gamma \quad . \quad (6)$$

$r_{av}$  is the average radius corresponding to  $\gamma$  layers. In this model, the pressure  $\sigma_r^*$  acts on the first of the remaining unstressed layers. The next step is to find the pressure on the spool. If we assume that the unstressed part of the winding reacts against the pressure  $\sigma_r^*$  like an elastic body, it can be shown that the pressure on the spool surface is

$$\sigma_r^* \cong 1.54 \sigma^* \quad . \quad (7)$$

$\sigma_r^*$  increases with increasing total thickness of the winding; however, the limit  $1.54 \sigma^*$  is reached soon.

We made experiments with a "race track" shaped coil similar to those which we intended to be used for the IMP quadrupole winding. The coil spool was divided in two parts (Fig. 5), and a load cell was provided in order to measure the force exerted by the winding. A tension of 52 lb was used during the winding process. The compound conductor consisted of multistrand NbTi in a copper matrix with  $0.057 \times 0.114$  in. cross section. A spiral wrap of  $0.080$  in.  $\times$   $0.005$  in. "Nomex paper" has been applied to the conductor for insulation. Approximately 50% of the conductor surface was exposed. Figure 6 shows the load cell force vs number of layers. After an approximately linear increase the force becomes almost constant, i.e., additional layers do not increase the force on the spool. The decreases in the magnitude of force as indicated at several places in Fig. 6 are due to interruptions of the winding process for making splices and repairing spots of damaged insulation.

Other measurements of the mechanical winding performance were made with a test apparatus called "coil expander" which is described in Ref. 1. These tests showed that appreciable differences can be expected between the actual performance of the coil winding volume under stress and the performance of an elastic body of identical shape which is exposed to the same volume forces. However, the elastic body model for a winding is at least a very important guideline for the stress analysis in coil winding.<sup>5</sup>

A much simpler approach for approximate stress calculations of axisymmetrical coils considering the electromagnetic forces due to the self-field can be achieved by assuming that the displacement vector  $\vec{u}$  has one constant magnitude for the entire coil volume. Furthermore, end effects have been neglected. A similar method has been described by Appleton, Cowhig, and Caldwell.<sup>6</sup> We made such calculations for several typical cases, and we found reasonable agreement with the stricter elastic model computations. However, none of these methods were sufficient to the stress analysis of the windings and structures of the IMP quadrupole system and, as it has been mentioned before, it was necessary to use additional special approximation methods.

Another major effort in the design of IMP has been toward the selection of an adequate superconductor. We have very carefully studied the use of multifilament NbTi in copper with current densities of about  $10\,000$  A/cm<sup>2</sup>. However, encouraged by the work of Sampson,<sup>2</sup> we have undertaken a parallel study program to determine if a higher current density ( $\sim 15\,000$  A/cm<sup>2</sup>) Nb<sub>3</sub>Sn design would provide a more reliable quadrupole coil system. Since the data are not yet complete for the Nb<sub>3</sub>Sn alternative, the following discussion will be limited to the NbTi coil system.

The central question in the design of an appropriate superconductor is that of the electrical stability of the conductor in the magnet system. Early attempts to use superconductors in mirror-quadrupole systems indicated the presence of electrical instabilities which are more severe than in axisymmetrical magnet systems. We have purchased a variety of superconducting samples from several manufacturers and subjected each sample to both short sample and coil tests to evaluate the stability of the various conductor designs. In general, we have found that the conductor performance seems to depend principally upon the conductor design rather than the special

---

5. R.W. Kilb and W.F. Westendorp, General Electric Co., Report No. 67-C-440 (1967).

6. A.D. Appleton, T.P. Cowhig, and J. Caldwell, in Proc. 2nd Intern. Conf. Magnet Technology, Oxford, 1967, p. 553.

manufacturing process. In testing the conductors, we have attempted to answer the following questions:

- 1) What influence has the copper/superconductor ratio?
- 2) What effect is found with smaller superconductor filaments?
- 3) Does the shape of the short sample curve, in the current sharing region (determined with constant field and variable current), relate to the performance of the conductor in a coil?
- 4) What conductor configurations show flux jumps in short sample tests (determined with constant current and variable field), and what effects do they have on coil performance?
- 5) Is the normal state surface cooling rate ( $W/cm^2$ ) a reasonable coil design parameter?

These questions have been examined primarily through the analysis of the results obtained with two standardized test methods which we have developed for short sample and coil performance. It has not been possible to find final answers to the questions listed, but the results of our tests show some influence of these effects and serve as a guide in selecting conductor.

The basic conductor shown in Fig. 7 was selected for our study. It is rectangular rather than square or round to facilitate good winding and to withstand most effectively the high electromagnetic forces in mirror quadrupole systems. The figure indicates 15 superconducting filaments; actually, our test samples contained as many as 252 filaments in this size conductor. Insulation is provided by a 50% coverage of Dupont Nomex paper 0.005 in. thick x 0.080 in. wide. The Nomex paper was selected after compressive displacement tests showed that under electromagnetic forces it allows less motion of the magnet windings than Mylar. However, the Nomex paper has a much lower shear strength than Mylar which must be provided for by the coil construction. The compressive displacement test also establishes the maximum winding section dimension which can be used without the danger that certain conductor loops become dislocated into void winding spaces resulting from electromagnetic forces.

The standard short sample test developed at ORNL uses the sample holder shown in Fig. 8. With this apparatus the conductor is suspended in free flowing liquid helium and is subjected only to hoop stresses due to the sample current and applied field. The test employs a very low impedance power supply so complete test cycles can be safely performed. The critical current, the region of current sharing, the normal state transition, and the recovery to the superconducting state can be measured. Our facility allows the test to be run in fields up to 75 kG and at sample currents up to 3000 A.

The standard coil test utilizes approximately 1000 ft of conductor wound into two identical coils which are operated in series-cusp mode as shown in Fig. 9. They are tested with a horizontal axis in the vertical field of a large 6 MW copper magnet which produces a homogeneous background field of up to 60 kG. As indicated, the peak forces are axially outward at the bottom of the coil, and axially inward at the top. The maximum field is found in the winding section near the midplane. The cusp coil test has been selected as that which best reproduces the extreme forces and field gradients of the mirror-quadrupole system. It also allows measurements over a wide range of magnetic fields and in a thermal environment which closely simulates that of the final IMP coils. Figure 10 shows an actual cusp coil after testing. Note the heavy series 310 stainless-steel structure required to restrain the forces generated by the cusp coil. Preliminary tests showed that perforated interlayer insulation sheet did not influence

the critical current or the charge rate sensitivity and therefore all tests were conducted with this additional insulation to avoid interlayer shear.

The results of these short sample and cusp coil tests are shown in Fig. 11. The data shown include the manufacturer of the conductor and the number of filaments (e.g., Supercon 18), the average filament diameter, the copper-to-superconductor ratio, test coil performance, and short sample performance.

Those parts of Fig. 11 which show test coil performance include the short sample  $I_c(H)$  for comparison (marked SS). As indicated by the parallel load lines, an externally applied background magnetic field of 0-60 kG is used to study the performance of the coil over a wide range of fields. Critical currents vary with the rate of current rise,  $dI/dt$ , in the test coil (e.g., the Supercon 18 coil reached  $I_c$  values from 550 A to 680 A, over the maximum field range 17 to 80 kG, when charged at 0.2 A/sec). At high charging rates (10 A/sec) the critical current was found to be relatively insensitive to the magnetic field.

Short sample tests of the conductors used in the coils are also shown in Fig. 11. In these tests, with a fixed background field of 0-75 kG, the sample current was increased beyond  $I_c$  into the current sharing region and then past the take-off current so that essentially all current was carried by the copper. Then, lowering the current, a copper resistance curve (marked 70, 60 and 50 kG) was determined. Finally, the recovery current was established as the temperature became low enough that the current returned to the superconductor.

The results of the short sample and coil tests lead to some tentative answers to the five conductor design questions which were listed above.

- 1) What influence has the copper/superconductor ratio?

Generally the samples with greater proportions of copper were more stable. However, exceptions are noted for those conductors with smaller filament diameters.

- 2) What effect is found with smaller superconductor filaments?

The coil with the smallest filament diameter (0.0030 in.) was found to be the most stable of those tested. It was possible to charge it at a rate of 1 A/sec (34 G/sec, maximum) to values very near short sample. With zero applied field, critical currents within 10% of short sample were measured at charging rates up to 10 A/sec. These results are in contrast to those obtained with the other test coils at zero applied field, all of which measured far below the short sample curve with fast charging rates. At slower charging rates, only the two cusp coils with conductors containing 0.0030 and 0.0111 in. filaments reached short sample performance over the full range of applied fields. The reason for the unusually good performance of the Supercon 15 coil is not clear, since a very similar Supercon 18 coil performed very differently.

- 3) Does the shape of the short sample curve, in the current sharing region (determined with constant field and variable current), relate to the performance of the conductor in a coil?

There seems to be a definite correlation on this point. Those conductors which exhibited smooth transitions into the current sharing region also behaved well in cusp coil tests. It is very likely that a smooth transition is necessary to allow continuous and steady dissipation of the trapped currents which are generated between filaments within a conductor by the increasing magnetic field. If the transition is not

smooth and reversible, the energy associated with the trapped current can be momentarily released causing  $T > T_c$  and the initiation of normal state propagation. Below the minimum propagation current (approximately given by the 10 A/sec performance line), temperature excursions above  $T_c$  are of little consequence since they do not initiate propagation.

- 4) What conductor configurations show flux jumps in short sample tests (determined with constant current and variable field), and what effects do they have on coil performance?

Short sample tests with fixed current and swept field operation show large flux jumps at low fields (5-10 kG) followed by a series of smaller flux jumps in the field range 10-45 kG in the Supercon 18, Cryomag 37 and Airco 85 conductors. The Supercon 15 conductor did not exhibit the large flux jumps at low fields but had the smaller flux jumps at higher fields. The Avco 252 sample did not show any flux jumps, suggesting that the filament diameter 0.0030 in. is sufficiently small to be stable in the manner suggested by a number of authors.<sup>7</sup> Those samples which showed large low field flux jumps performed poorly in coils. The smaller flux jumps at higher fields seem to have no detectable influence on coil performance.

- 5) Is the normal state surface cooling rate ( $W/cm^2$ ) a reasonable coil design parameter?

In our coil tests normal state transitions have been recorded over a range of currents which would correspond to 0.6 to 12  $W/cm^2$  surface dissipation if the current were completely in the copper. In partially stabilized coils, i.e., beyond 0.2 to 0.4  $W/cm^2$ , the surface cooling rate does not seem to be a sensible design parameter.

The test cusp coils have been operated up to short sample performance of 20 000  $A/cm^2$  at 60 kG. They have yielded complementary data to aid in the evaluation of short sample tests. In addition, using the information from these tests, we have wound and tested two 7 in. bore, 1 H mirror coils (Fig. 12) which employ 6000 ft of Supercon 15 conductor each. The performance of the mirror coils was predictable by the cusp coil tests. Each mirror coil reached short sample performance at 67 kG, 600 A ( $10^4 A/cm^2$ ) with 0.2 A/sec charging rate. With faster charging rates the critical current was degraded in quantitative agreement with cusp coil tests.

Figure 13 shows the entire IMP facility. The two mirror coils will be installed in the fall of 1968. It is expected that the complete magnet system (including the four quadrupole coils which surround the mirror coils) will be operational in 1969.

---

7. P.F. Chester, in Reports on Progress in Physics (The Institute of Physics and the Physical Society, London, 1967), Vol. 30, Part II, p. 561.

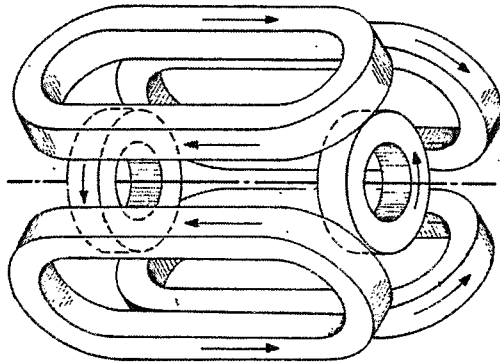


Fig. 1. Schematic of a B-minimum magnet system

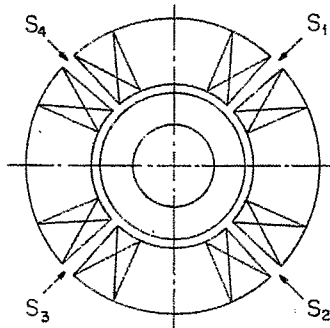


Fig. 2. Conceptual design of the IMP magnet system with wedge-shaped saddle coils forming symmetrical quadrupoles.

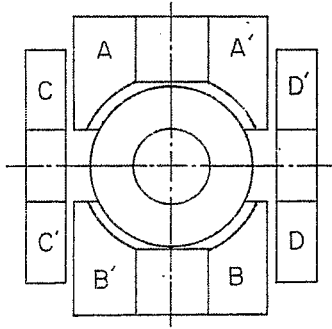


Fig. 3. Nonsymmetrical magnet system for IMP.

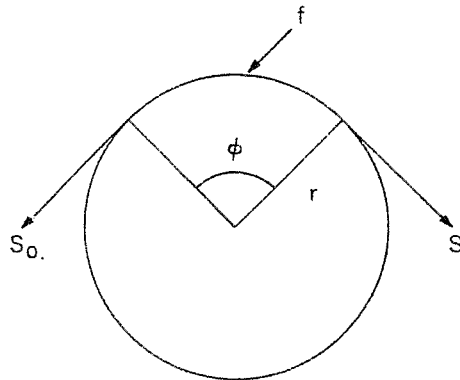


Fig. 4. Forces in a rope wound around a spool.

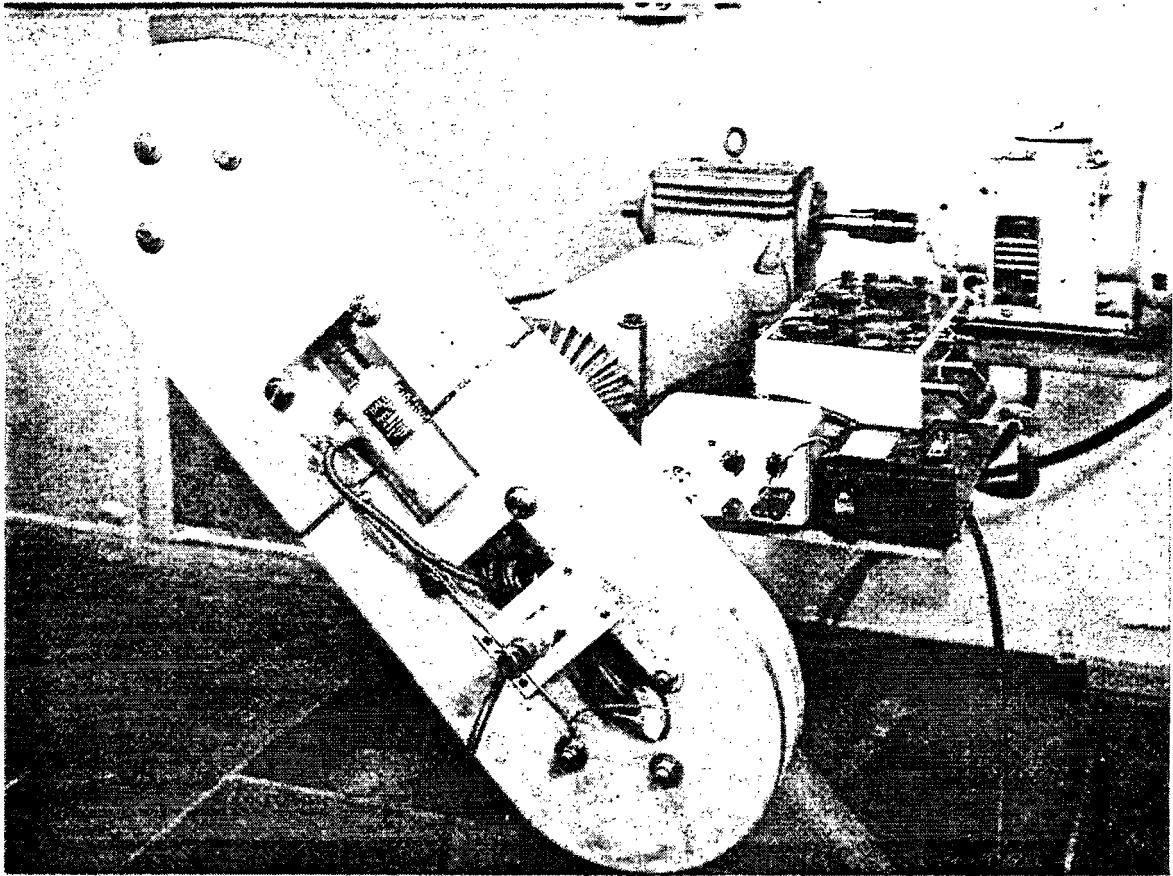


Fig. 5. Race track coil winding experiment.

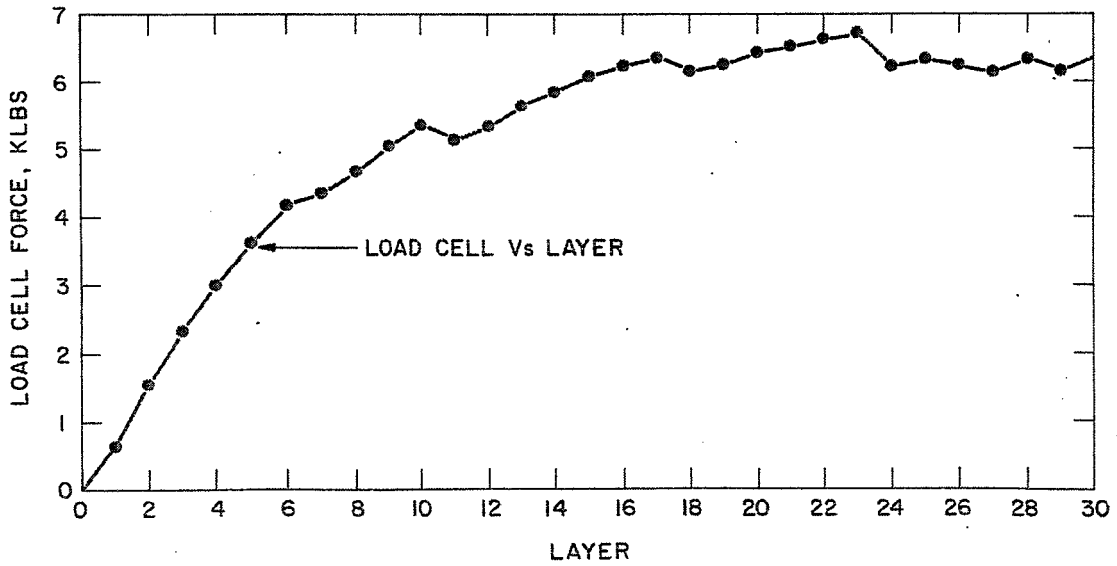


Fig. 6. Results of race track coil winding experiment.

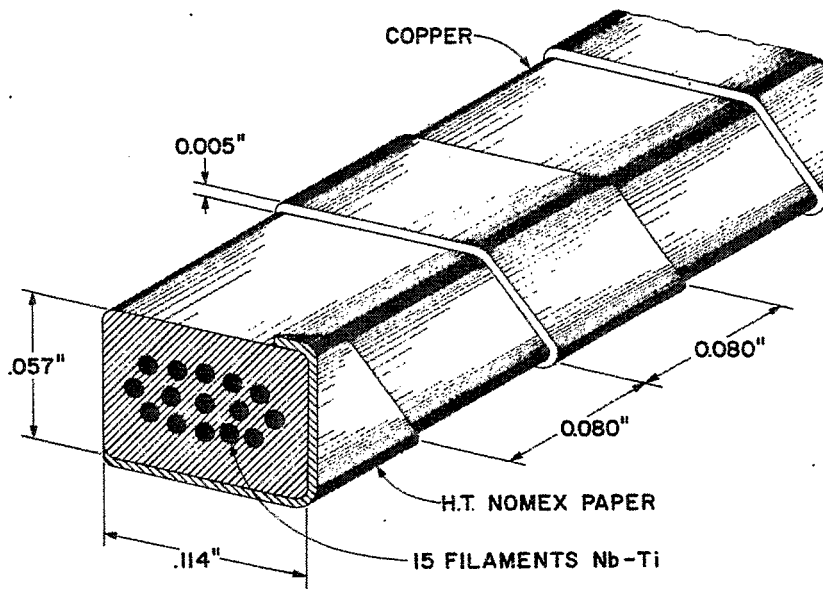


Fig. 7. IMP superconductor.

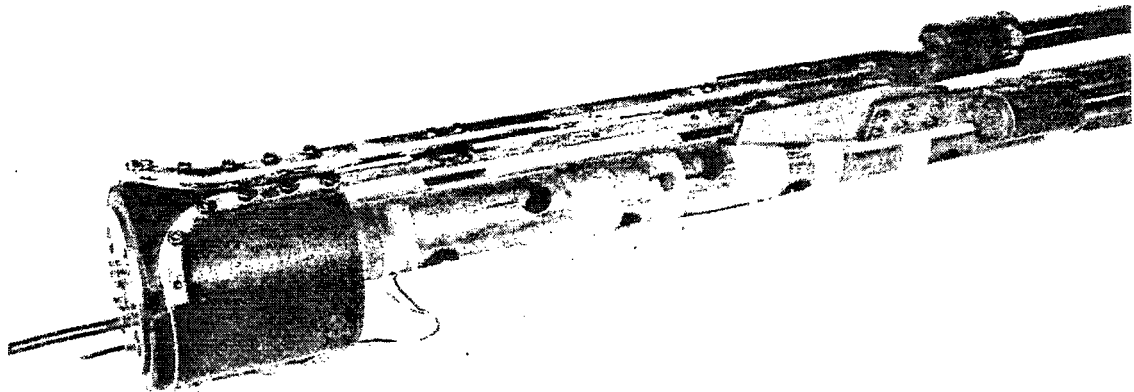


Fig. 8. Short sample test holder.

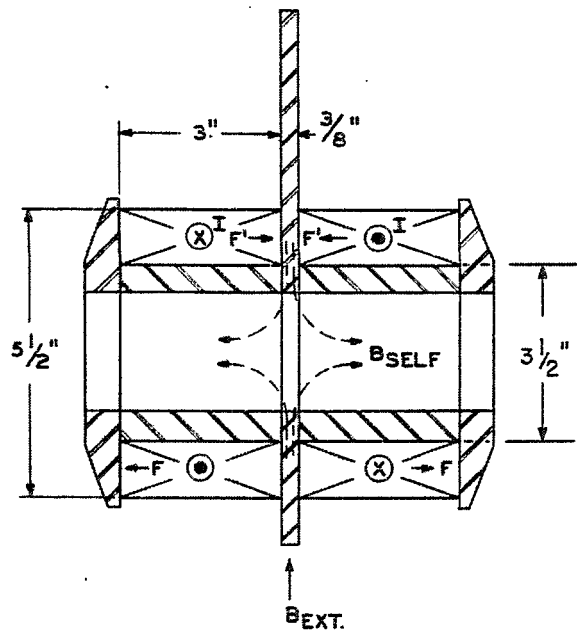


Fig. 9. Large cusp test coil.

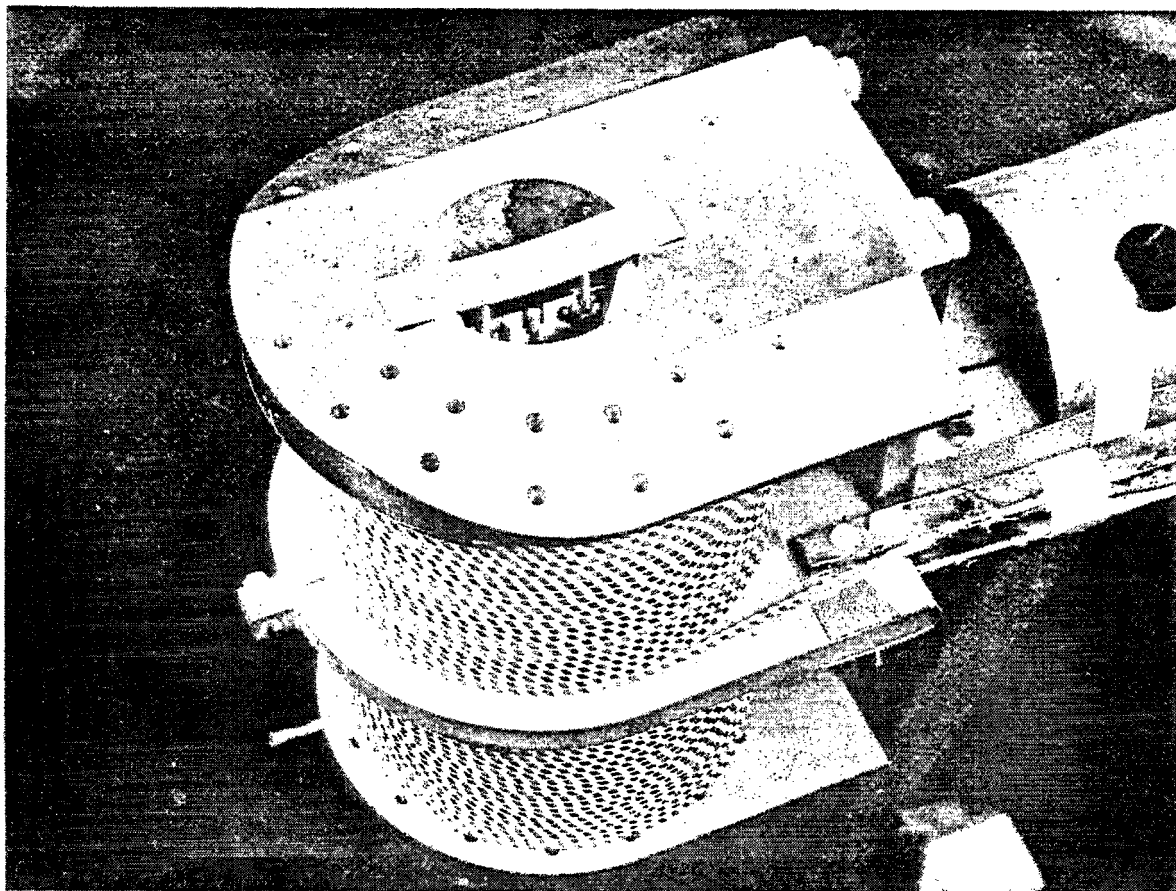


Fig. 10. Completed cusp test coil.

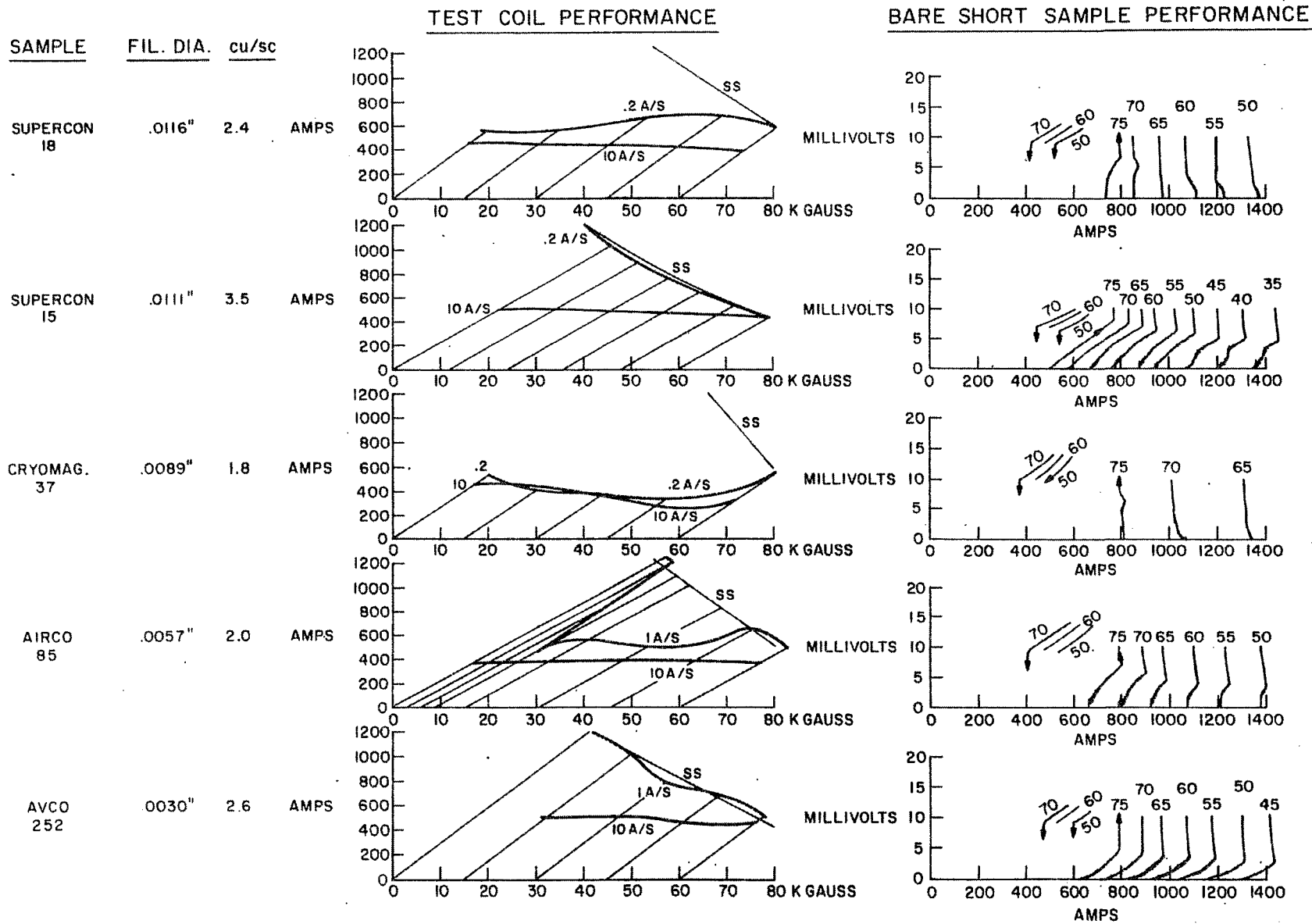


Fig. 11. Coil and short sample tests of 0.057 in. x 0.114 in. NbTi conductor.

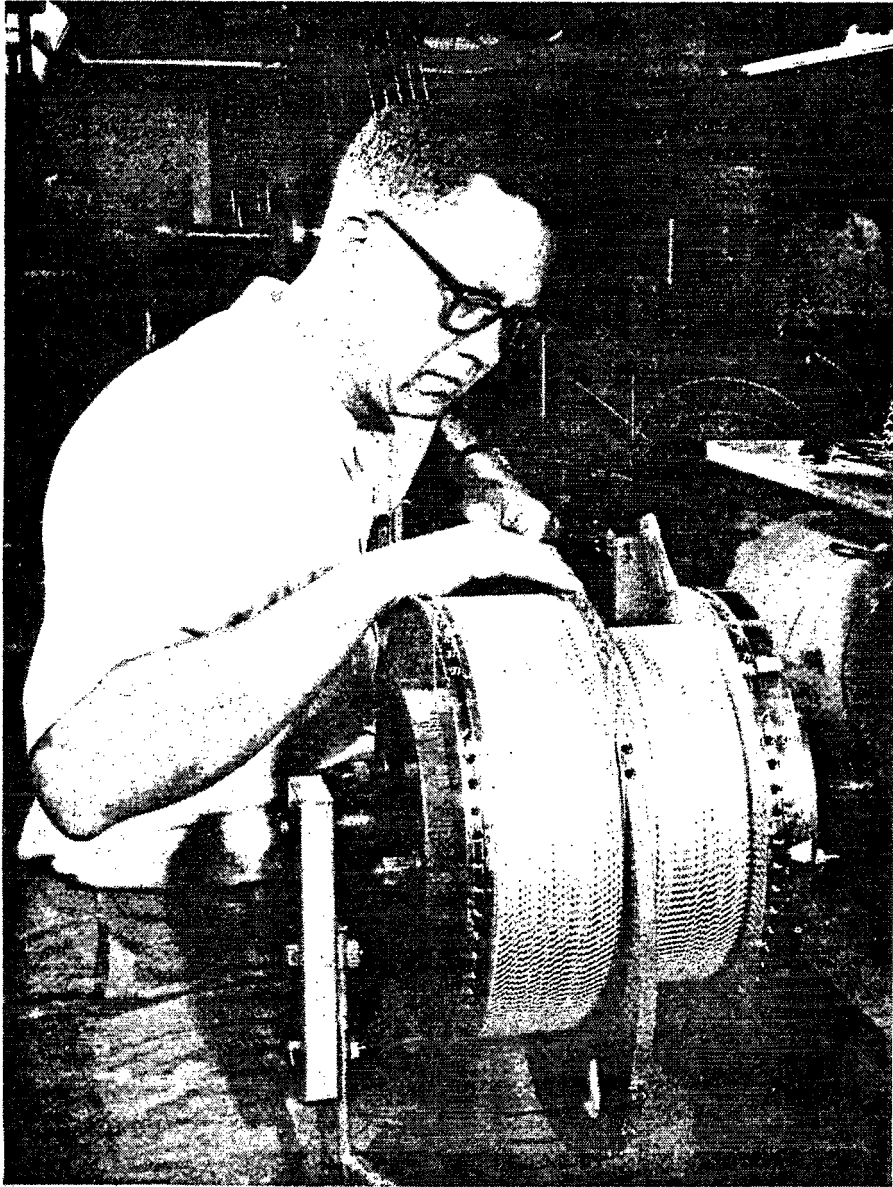


Fig. 12. IMP mirror coil A during winding.

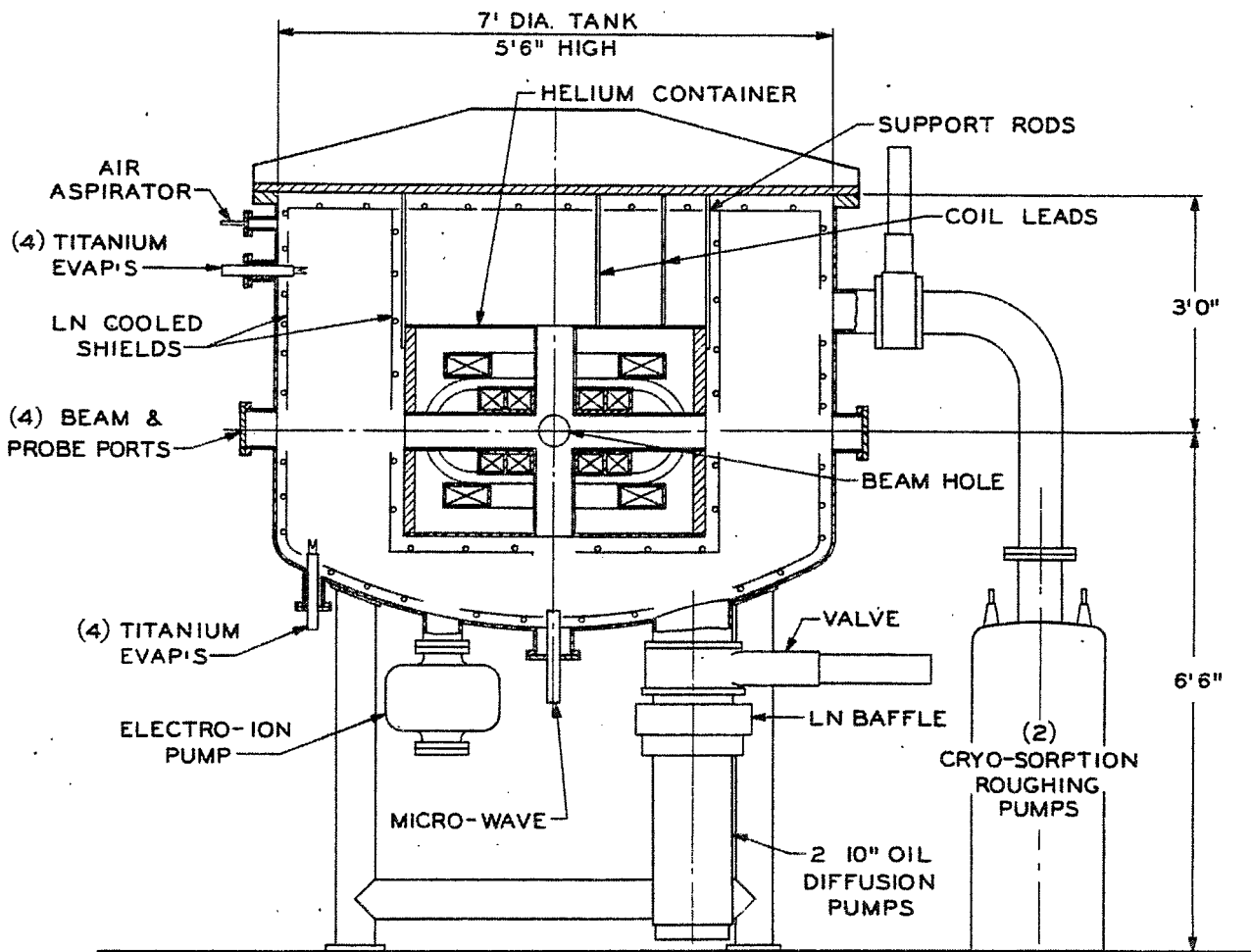


Fig. 13. IMP facility.